

# ABPP-CoDEL: Activity-Based Proteome Profiling-Guided Discovery of Tyrosine-Targeting Covalent Inhibitors from DNA-Encoded Libraries

Lulu Jiang,<sup>○</sup> Sixiu Liu,<sup>○</sup> Xinglong Jia,<sup>○</sup> Qinting Gong, Xin Wen, Weiwei Lu, Jintong Yang, Xinyuan Wu, Xuan Wang, Yanrui Suo, Yilin Li, Motonari Uesugi, Zhi-bei Qu, Minjia Tan,\* Xiaojie Lu,\* and Lu Zhou\*



Cite This: *J. Am. Chem. Soc.* 2023, 145, 25283–25292



Read Online

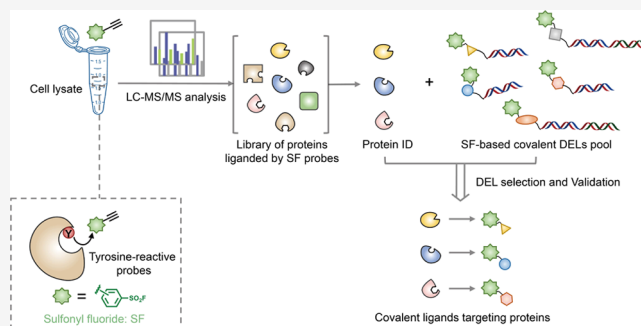
ACCESS |

Metrics & More

Article Recommendations

Supporting Information

**ABSTRACT:** DNA-encoded chemical library (DEL) has been extensively used for lead compound discovery for decades in academia and industry. Incorporating an electrophile warhead into DNA-encoded compounds recently permitted the discovery of covalent ligands that selectively react with a particular cysteine residue. However, noncysteine residues remain underexplored as modification sites of covalent DELs. Herein, we report the design and utility of tyrosine-targeting DELs of 67 million compounds. Proteome-wide reactivity analysis of tyrosine-reactive sulfonyl fluoride (SF) covalent probes suggested three enzymes (phosphoglycerate mutase 1, glutathione s-transferase 1, and dipeptidyl peptidase 3) as models of tyrosine-targetable proteins. Enrichment with SF-functionalized DELs led to the identification of a series of tyrosine-targeting covalent inhibitors of the model enzymes. In-depth mechanistic investigation revealed their novel modes of action and reactive ligand-accessible hotspots of the enzymes. Our strategy of combining activity-based proteome profiling and covalent DEL enrichment (ABPP-CoDEL), which generated selective covalent binders against a variety of target proteins, illustrates the potential use of this methodology in further covalent drug discovery.



## INTRODUCTION

Covalent drugs, also known as targeted covalent inhibitors, are a class of pharmaceuticals that form permanent bonds with disease-causing proteins, leading to prolonged target engagement and exceptional potency.<sup>1</sup> The unique pharmacological benefits of covalent drugs have prompted major pharmaceutical companies to continually develop them into the market or clinical trials, particularly in the areas of oncology and infectious diseases.<sup>2</sup> Notable examples of covalent drugs include afatinib, the first FDA-approved covalent EGFR inhibitor used as a first-line treatment of metastatic NSCLC with activating mutations in EGFR,<sup>2,3</sup> and ibrutinib, a BTK inhibitor approved for the treatment of mantle-cell lymphoma.<sup>4,5</sup> Furthermore, covalent modification of critical amino acids has allowed for the targeting of traditionally undruggable proteins, as demonstrated by sotorasib, an inhibitor of mutant KRAS (G12C) that has withstood decades of drug discovery efforts.<sup>6,7</sup>

Early examples of covalent drugs generally originated serendipitously from natural products. However, a more systematic and rational approach has gained popularity with the use of structure-guided rational design, where an electrophilic group is incorporated into a known reversible ligand. Another emerging approach is the screening of

chemical libraries containing electrophilic compounds.<sup>8–10</sup> This electrophile-centric screening strategy enables the direct identification of covalent ligands from the outset rather than designing them from known reversible ligands. Despite these significant advancements, the discovery of covalent drugs that target noncysteine residues remains challenging. Currently, clinically used covalent drugs primarily target critical cysteine,<sup>2</sup> with lysine,<sup>11</sup> serine,<sup>12</sup> and threonine<sup>13</sup> residues being targeted to a lesser extent. Covalent modification of other amino acids is even more difficult due to their low reactivity and high abundance on the protein surface. An alternative covalent conjugation strategy is essential when any of the cysteine or other reactive residues are not available in the protein of interest. One possibly targetable residue is tyrosine, which harbors a moderately reactive phenol group and is low abundance on the protein surface due to its relative

Received: August 14, 2023

Published: October 19, 2023



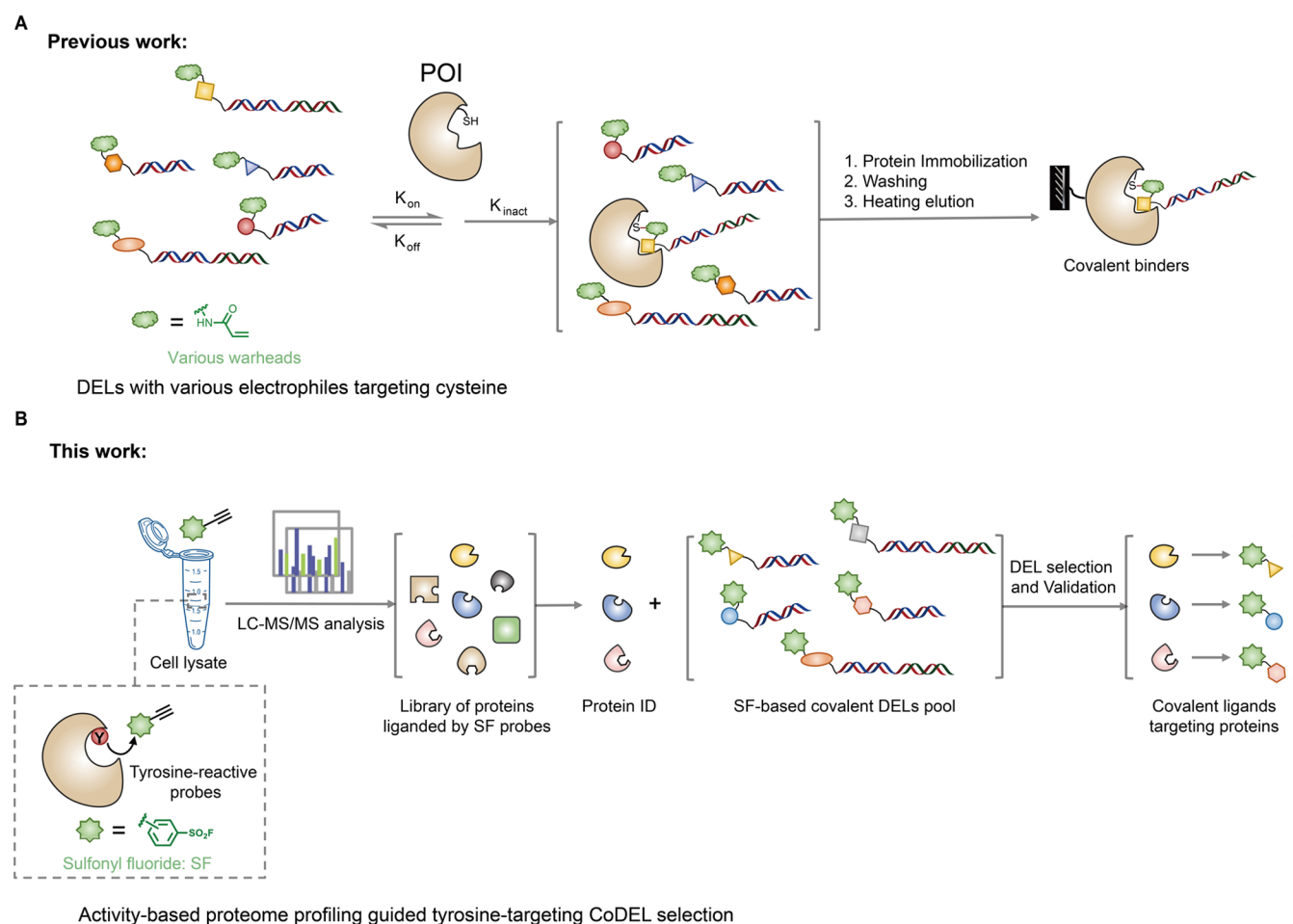


**Figure 1.** Proposed ABPP-CoDEL selection strategy. (A) CoDELs are always selected against proteins with functional cysteines. (B) The proposed ABPP-CoDEL selection method. The sulfanyl fluoride-based probes are used to identify the probe-modified proteins that are selected for SF-based CoDEL selection. After washing out, the hit compounds are encoded, of which the model of action is next validated.

hydrophobicity. The development of tyrosine-selective covalent ligands would complement the existing strategies for covalent ligand discovery or design.

The DNA-encoded chemical library (DEL) has emerged as a powerful technology for rapidly synthesizing and selecting library members.<sup>14–17</sup> DELs incorporating an electrophile warhead, known as covalent DELs, have been utilized for covalent drug discovery.<sup>14</sup> Winssinger and co-workers pioneered the use of PNA-encoded electrophilic peptide libraries for diverse protein targets, including protease,<sup>18–20</sup> MEK2,<sup>21</sup> ERBB2,<sup>21</sup> and bromodomains.<sup>22</sup> Large covalent DELs have been screened against a wide range of protein targets, such as BTK,<sup>23,24</sup> JAK1,<sup>24,25</sup> Pin1,<sup>24</sup> and SARS-CoV-2,<sup>26</sup> leading to the identification of unique covalent ligands. However, the use of these covalent DELs has been limited to targeting cysteine or serine residues, primarily due to the poor diversity of warheads used such as acrylamide, acrylate, ketone, epoxide, and boronic acid (Figure 1A). Therefore, the development of covalent DELs with noncysteine-targeting warheads would expand the utility of DELs for the discovery of novel covalent inhibitors.

In this study, we report the discovery of covalent ligands that target tyrosine residues from sulfanyl fluoride (SF)-functionalized DNA-encoded chemical libraries. Our platform integrates activity-based protein profiling (ABPP) of SF-based covalent probes with an enrichment of the SF-functionalized

DELs, providing a generalizable workflow for discovering tyrosine-targeting covalent ligands (Figure 1B). Through the screening of a vast DELs pool containing 67 million compounds, we identified novel covalent ligands that selectively target tyrosine residues in phosphoglycerate mutase 1 (PGAM1), glutathione s-transferase 1 (GSTP1), and dipeptidyl peptidase 3 (DPP3), respectively. This demonstration highlights the potential of sulfanyl fluoride as a promising warhead for tyrosine-targeting covalent ligands and the importance of combining activity-based proteome profiling and covalent DEL enrichment (ABPP-CoDEL) in the rapid discovery of covalent inhibitors.

## RESULTS AND DISCUSSION

**Chemical Proteomic Evaluation of Sulfanyl Fluoride-Based Covalent Probes.** We chose sulfanyl fluoride (SF) as the warhead for developing tyrosine-selective covalent ligands, given that SF has increasingly been used in chemical biology and molecular pharmacology investigations due to its ability to react with tyrosine residues.<sup>27–31</sup> However, the sensitivity of SFs to tyrosine residues can vary in different protein microenvironments, and randomly selecting target proteins containing tyrosine residues may impact the efficiency of subsequent screening steps. To identify proteins suitable as targets of tyrosine-targeting covalent ligands, we initially conducted an activity-based protein profiling (ABPP)<sup>32–35</sup>

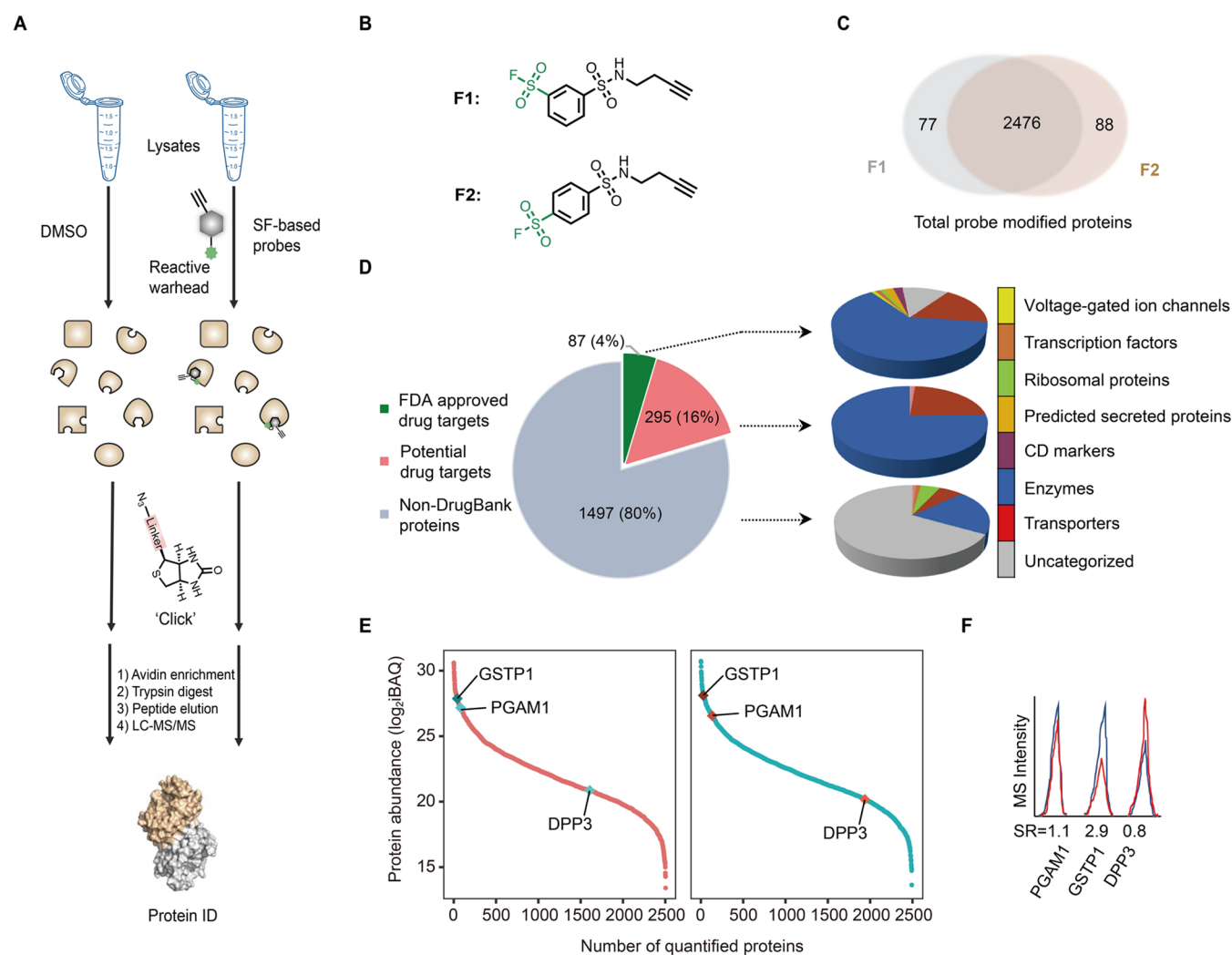


**Figure 2.** Analysis of proteins liganded by sulfonyl fluoride electrophiles. (A) General protocol for LC-MS/MS workflow to identify proteins liganded by SF-based probes. (B) Chemical structures of sulfonyl fluorides F1 and F2, respectively. (C) Comparison of F1- and F2-modified proteins identified from cell proteomes (HEK293T) treated with SF probes (250  $\mu$ M, 1 h, 25  $^{\circ}$ C). (D) Fraction of liganded proteins found in DrugBank (left). Functional classes of FDA-approved drug targets, potential drug targets, and nondrug targets (right). (E) Abundance of quantified proteins liganded by F1 (left) and F2 (right) using a label-free quantitative proteomics analysis. Whole cell lysates of HEK293T were treated for 1 h with 250  $\mu$ M F1 and F2, respectively, followed by CuAAC and label-free quantitative proteomics analysis. Three proteins selected for further DELs selection were indicated. (F) The nucleophilicity of PGAM1, GSTP1, and DPP3 with F1 was determined by using the area under the curve of MS1 extracted ion chromatograms (EIC) to quantify the result SILAC ratios (SR). SILAC-labeled light and heavy whole cell lysates were treated for 1 h with 25  $\mu$ M and 250  $\mu$ M F1, respectively, before being mixed, followed by CuAAC and quantitative proteomics analysis. Protein reactivity was segregated into low, medium, and high groups based on their respective SILAC ratios ( $SR > 5$ ,  $2 < SR \leq 5$ ,  $SR \leq 2$ ).

experiment using SF-based covalent probes to systematically assess the accessibility and reactivity of proteomes (Figure 2A).

The design of the SF-based probes is depicted in Figure 2B. To incorporate an alkyne reporter tag for downstream detection, we synthesized alkyne-modified sulfonyl fluoride probes, F1 and F2, by coupling 1-amino-3-butyne to 3 or 4-(chlorosulfonyl)benzenesulfonyl fluorides. During the construction of the covalent DEL, we found that ortho-substituted SF was susceptible to reacting with amino or hydroxyl groups intramolecularly in the parent compounds. Thus, the synthesis and subsequent experiments of the ortho-substituted SF probe were not performed. Subsequently, we evaluated the reactivity of these probes for proteome profiling. In-gel fluorescence analysis of HEK293T cell proteomes demonstrated robust proteome labeling by F1 and F2 in a concentration- and time-dependent manner (Figure S1).

We also analyzed the identities of the labeled proteins. HEK293T cell proteomes were treated with F1 and F2 (250  $\mu$ M, 1 h, 25  $^{\circ}$ C) followed by coupling with a biotin-azide conjugate via copper-catalyzed azide-alkyne cycloaddition (CuAAC). The biotin-labeled proteomes were then enriched by avidin affinity chromatography and digested with trypsin protease. The released peptides were subsequently sequenced using high-resolution liquid chromatography–mass spectrometry (LC-MS/MS). Approximately 2400 proteins labeled separately by F1 and F2 were identified (Figure 2C). Around 20% of them were protein targets of FDA-approved or potential drugs, according to the DrugBank database<sup>36</sup> (Figure 2D). The DrugBank proteins labeled by SF probes originated from diverse functional classes that are regarded as druggable, primarily enzymes (Figure 2D). The dynamic range of the labeled proteome was examined next by quantitative proteomics. We focused on three enzymes (phosphoglycerate

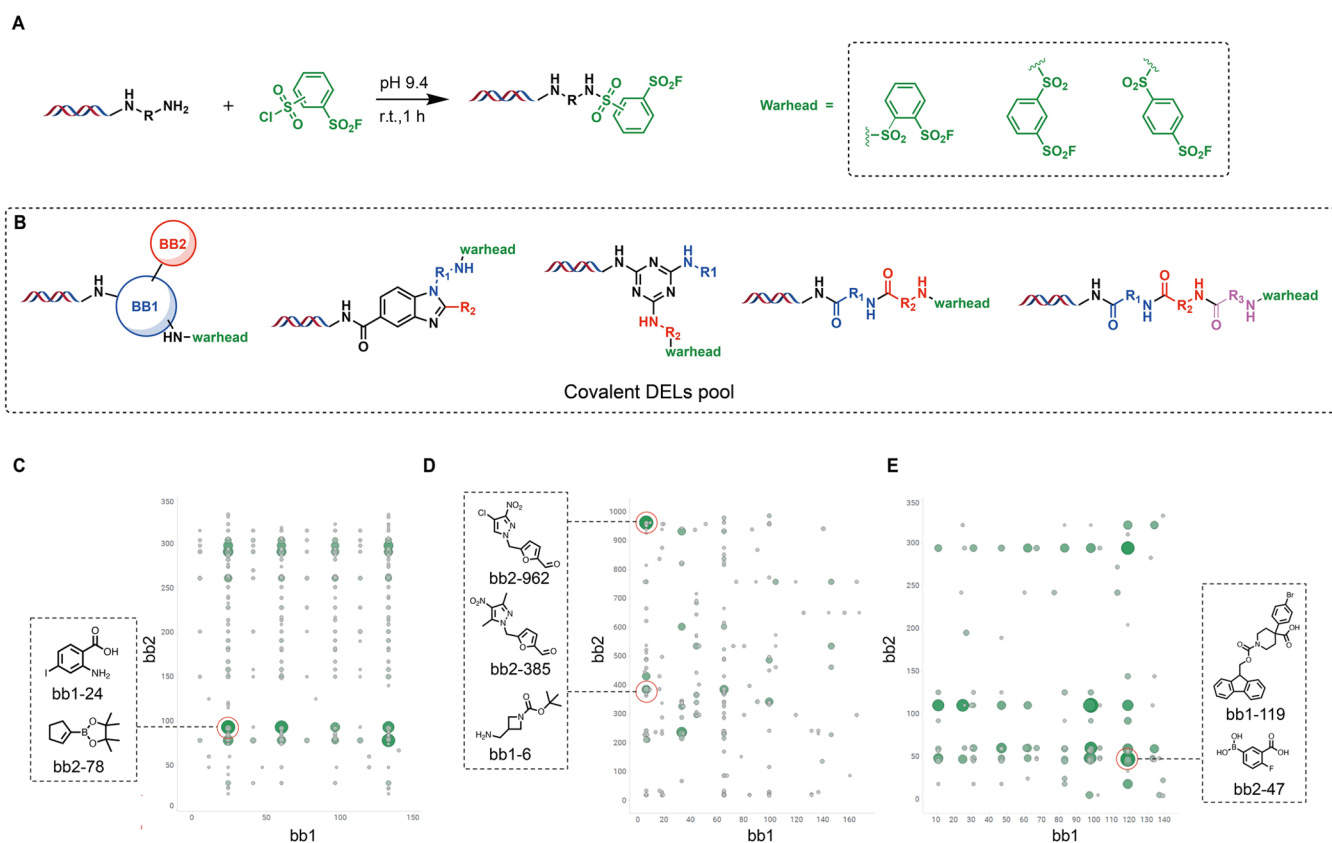


**Figure 3.** SF-based CoDEL pool selection against target proteins. (A) Synthesis of the covalent DNA-encoded library. (B) Structures of selection libraries. (C–E) Scatter plot of libraries with preferred scaffolds and the corresponding structural features, where each axis represents one cycle of chemistry, and the size of each dot is proportional to the copy counts of a unique compound. Selection data analysis of DEL01B for PGAM1 (C) and DPP3 (E), and DEL02B for GSTP1 (D). The building blocks with high fold-enrichment are highlighted.

mutase 1 (PGAM1), glutathione *s*-transferase 1 (GSTP1), and dipeptidyl peptidase 3 (DPP3)) for subsequent DEL screening as examples according to their different types of catalytic functions including isomerase, transferase, and hydrolase. These three enzymes that harbor reactive hotspot tyrosines amenable to sulfur-triazole exchange (SuTEx) reaction<sup>33</sup> showed high (PGAM1 and GSTP1) and low (DPP3) protein abundance (Figure 2E).

To directly evaluate the reactivity of F1 for each enzyme, we conducted SILAC (stable isotope labeling with amino acids in cell culture)-based quantitative proteomics. The SILAC-labeled light (<sup>12</sup>C<sub>6</sub> lysine and <sup>12</sup>C<sub>6</sub><sup>14</sup>N<sub>4</sub> arginine) and heavy (<sup>13</sup>C<sub>6</sub> lysine and <sup>13</sup>C<sub>6</sub><sup>15</sup>N<sub>4</sub> arginine) whole cell lysates were treated with 25 and 250 μM F1 for 1 h, respectively. After sample mixing and the CuAAC click reaction, the biotin-labeled proteins were enriched via avidin affinity chromatography and subjected to quantitative proteomics analysis via LC-MS/MS analysis. The results confirmed a high reactivity of F1 for PGAM1 (SILAC ratio: ~ 1.1), DPP3 (SILAC ratio: ~ 0.8), and a medium reactivity for GSTP1 (SILAC ratio: ~ 2.9) (Figure 2F).

**Construction and Screening of Sulfonyl Fluoride-Based Covalent DELs.** We set out to select SF-based covalent DNA-encoded libraries (SF-based DELs) to identify covalent ligands targeting the three proteins. To validate the suitability of SF-based DELs as a source of tyrosine-targeting covalent ligands, we generated diverse chemical libraries of millions of structures after testing the stability of sulfonyl fluoride electrophiles under DNA-compatible reaction con-

ditions (Figures 3A,B and S2–S5). A reversible DEL pool without the sulfonyl fluoride warhead was also prepared as a control. Among the libraries, DEL01 was chosen as an example, as illustrated in Figure S6. In DEL01, Fmoc-amino acid and 4-amino-benzoic acid building blocks (referred to as bb1) were acylated onto the primary amine of the oligonucleotide headpiece at cycle 1. After pooling and deprotection of N-Fmoc, the cycle 1 product was coupled to 327 boronic acid building blocks in cycle 2 (bb2) via the Suzuki coupling reaction. Finally, all building blocks were terminated with a sulfonyl fluoride group through a nucleophilic aromatic substitution (S<sub>N</sub>Ar) reaction with chlorosulfonyl-benzenesulfonyl fluorides.

For screening, we followed the previously reported covalent selection method.<sup>24</sup> Briefly, proteins were incubated with the 2.5 nmol covalent DEL pool, composed of a total of 67 million compounds in PBS. The 6 × his-tagged recombinant PGAM1, GSTP1, and DPP3 were then immobilized on the Ni-NTA beads matrix, respectively. After one round of enrichment, the enriched pools were subjected to PCR amplification and NGS sequencing. Analysis of these data revealed several features in the irreversible DEL pool but not in the reversible DEL pool. In the 2D plot, one dot represents one on-DNA compound constructed by two cycles of building blocks, which provided one highly enriched cluster (Figure 3C–E). The plot of sequence counts revealed the preferential enrichment of bb1-24/bb2-78 pairs for PGAM1 in DEL01B, bb1-6/bb2-385 pairs for GSTP1 in DEL02B (see Figure S7 for construction of DEL02), and bb1-119/bb2-47 pairs for DPP3 in DEL01B with

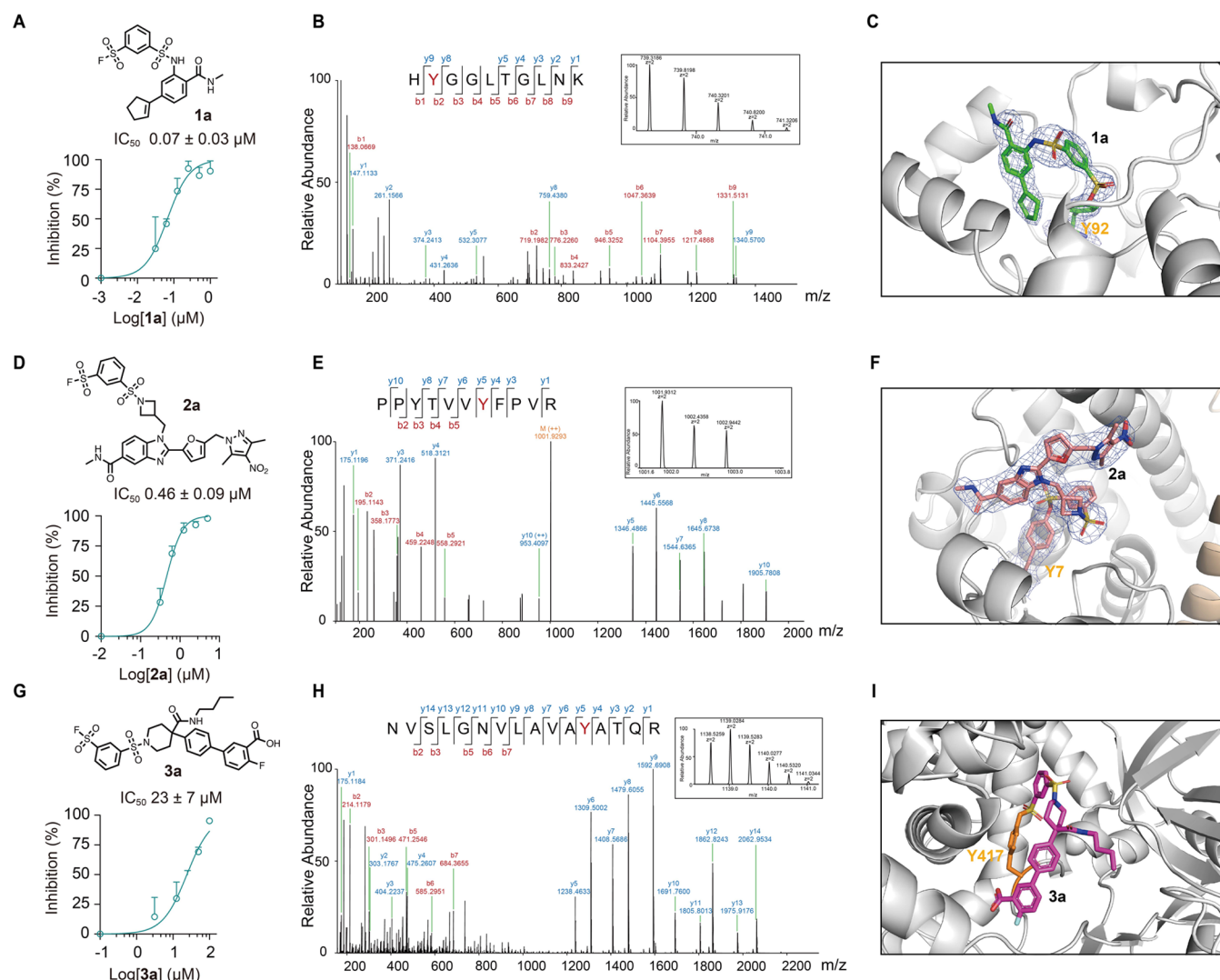


**Figure 4.** Validation of hit compounds with target proteins. (A) Top: Chemical structure of hit compound **1a**. Bottom:  $IC_{50}$  value of **1a** against recombinant PGAM1. Data represent average values  $\pm$  s.d.,  $n = 3$  per group. (B) Annotated MS2 fragmentation spectra analysis of **1a** with recombinant PGAM1 (0.1 mM). Modification of Tyr 92 at the catalytic site is highlighted in red. (C) Crystal structure of **1a** bound to PGAM1 (PDB ID code 7XB7) at a resolution of 2.20 Å. The PGAM1 (gray) is shown as cartoon, and **1a** (green) as sticks. (D) Top: Chemical structure of **2a**. Bottom:  $IC_{50}$  value of **2a** against recombinant GSTP1. Data represent average values  $\pm$  s.d.,  $n = 3$  per group. (E) Annotated MS2 fragmentation spectra analysis of **2a** with recombinant GSTP1 (0.1 mM). Modification of Tyr 7 at the catalytic site is highlighted in red. (F) Crystal structure of **2a** bound to GSTP1 (PDB ID code 7XBA) at a resolution of 2.83 Å. The GSTP1 (gray) is shown as cartoon, and **2a** (pink) as sticks. (G) Top: Chemical structure of **3a**. Bottom:  $IC_{50}$  value of **3a** against recombinant DPP3. Data represent average values  $\pm$  s.d.,  $n = 3$  per group. (H) Annotated MS2 fragmentation spectra analysis of **3a** with recombinant DPP3 (0.1 mM). Modification of Tyr 417 at the noncatalytic site was highlighted in red. (I) Docking experiment to predict the binding mode of **3a** with DPP3 (PDB ID code 3FVY). The DPP3 (gray) is shown as cartoon, and **3a** (purple) as sticks.

the high fold-enrichment of 47.35, 90.38, and 18.49, respectively (Figure 3C–E).

Resynthesis of the highly coenriched compounds (off-DNA) yielded **1a**, **2a**, and **3a** as the hit compounds for further functional studies. Compounds **1a** and **2a** inhibited the enzymatic activity of PGAM1 and GSTP1 with  $IC_{50}$  values of 70 and 460 nM, respectively (Figure 4A,D). On the other hand, compound **3a** engaged DPP3 with a higher  $IC_{50}$  value of 23  $\mu$ M (Figure 4G). To examine the liganded amino acid sites of target proteins, we treated recombinant PGAM1, GSTP1, and DPP3 with **1a**, **2a**, and **3a** (3-fold excess of the compound, 12 h, 25 °C), respectively, and evaluated the reaction products by the tandem mass spectrometry analysis. The fragment ions (y and b) indicated Tyr 92 of PGAM1 as the reaction site of **1a** (mass adduct of 418.07 Da), Tyr 7 of GSTP1 as that of **2a**

(mass adduct of 665.14 Da), and Tyr 417 of DPP3 as that of **3a** (mass adduct of 600.14 Da) (Figure 4B,E,H).

To gain insights into the binding mode, we cocrystallized PGAM1 complexed with **1a**. The structure was determined by X-ray crystallography at a resolution of 2.20 Å, followed by molecular replacement and structure refinement (Supplementary Table 2). The structure showed a sulfonate ester bond formed between the sulfonyl group of **1a** and the hydroxyl group of Tyr 92, a substrate binding site of PGAM1 (Figures 4C and S9). The O atom of the newly created sulfonate ester bond interacted with the amino group of Asn 188 and the phenyl-cyclopentene group of **1a** inserted into the hydrophobic pocket of PGAM1 to create  $\pi$ – $\pi$  interaction with Phe 22, Leu 95, Val 112, and Trp 115 (Figure S12A). The structure of the GSTP1–**2a** complex was also determined by X-ray

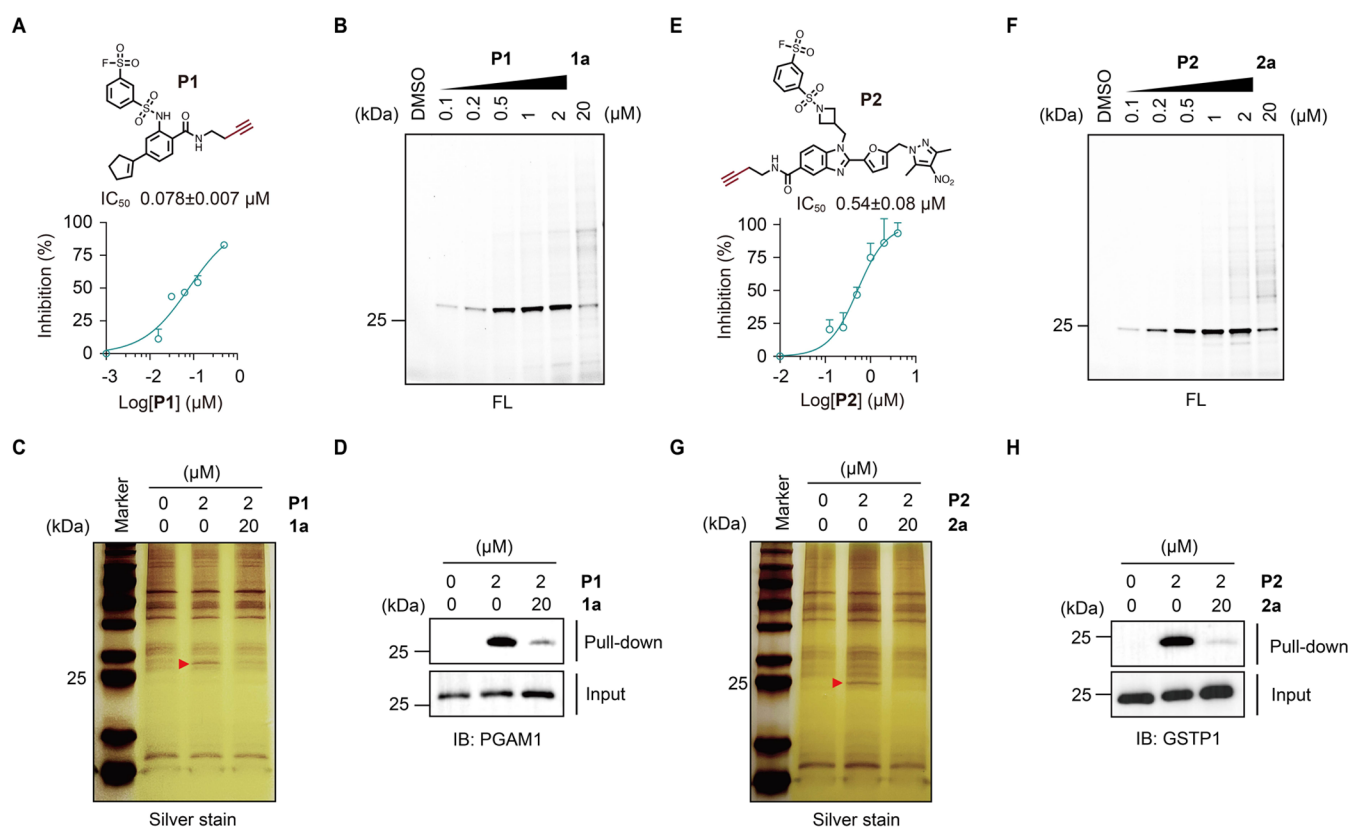


**Figure 5.** Target selectivity validation of hit compounds. (A) Top: Chemical structure of an alkyne-modified probe **P1**. Bottom:  $IC_{50}$  value of **P1** against recombinant PGAM1. Data represent average values  $\pm$  s.d.;  $n = 3$  per group. (B) Concentration-dependent labeling profiles of HEK293T cell lysates with **P1** and competitive labeling profiles with **P1** ( $2 \mu\text{M}$ ) in the presence of **1a** ( $20 \mu\text{M}$ ). FL: in-gel fluorescence scanning. (C) Pull down and silver staining results in the presence or absence of **1a**. (D) Target validation of PGAM1 by pull down and Western blotting in the presence or absence of the corresponding competitor **1a**. (E) Top: Chemical structure of probe **P2**. Bottom:  $IC_{50}$  value of **P2** against recombinant GSTP1. Data represent average values  $\pm$  s.d.;  $n = 3$  per group. (F) Concentration-dependent labeling profiles of HEK293T cell lysates with **P2** and competitive labeling profiles with **P2** ( $2 \mu\text{M}$ ) in the presence of **2a** ( $20 \mu\text{M}$ ). (G) Pull down and silver staining results in the presence or absence of **2a**. (H) Target validation of GSTP1 by pull down and Western blotting in the presence or absence of **2a**.

crystallography analysis (Supplementary Table 2). The cocrystal structure at a resolution of  $2.83 \text{ \AA}$  showed a new sulfonate ester bond formed between **2a** and Tyr 7, a key catalytic residue of GSTP1 (Figures 4F and S10). The O atom of the sulfonamide group interacted with the amino group of Gln 51, while the benzimidazolfuran scaffold was inserted into the hydrophobic pocket around Phe 8, Val 10, Val 35, Ile 104, and Tyr 108 (Figure S12B).

Unfortunately, we were unable to obtain cocrystals of DPP3 and **3a**. Thus, we determined the labeling efficiency of tyrosine residues in DPP3 following treatment with **3a**. The result demonstrated that **3a** reacted with Tyr 417 in a high ratio (71%) which supported that **3a** did react with Tyr 417 of DPP3 (Figure S11A). Tyr 417 is not a catalytic site of DPP3, and its mutation has no significant impact on the DPP3 enzymatic activity.<sup>33</sup> Nevertheless, a docking model showed that Tyr 417 is close to its substrate binding pocket. The covalent reaction of Tyr 417 with **3a** may disrupt the substrate binding or the conformation change of DPP3 during substrate binding (Figures 4I, S11, and S12C).

These results demonstrate that **1a**, **2a**, and **3a** are novel tyrosine-targeting covalent inhibitors against PGAM1, GSTP1, and DPP3, respectively. Compounds **1a** and **2a** targeted the catalytic tyrosines in the substrate binding pockets (Tyr 92, PGAM1; Tyr 7, GSTP1), and **3a** reacted with the noncatalytic Tyr 417 to inhibit the activity of DPP3. Our results

demonstrate the feasibility of discovering tyrosine-targeting covalent inhibitors by combining the proteome reactivity profiling of SF-based probes and the screening of SF-based covalent DELs.

**Selective Target Engagement of the Covalent Ligands.** To further validate the selectivity of ligands, we designed and synthesized probes **P1** (Figure 5A) and **P2** (Figure 5E) by adding an alkyne reporter tag to the methyl group of **1a** and **2a** for downstream click chemistry. HEK293T cell proteomes were treated with probe **P1** and **P2** ( $2 \mu\text{M}$ , 2 h,  $25 \text{ }^\circ\text{C}$ ) followed by CuAAC coupling with rhodamine-azide conjugate and analyzed by SDS-PAGE. In-gel fluorescent imaging showed  $\sim 27$  and  $\sim 25$  kDa bands in the samples treated with **P1** and **P2**, respectively, in a concentration-dependent manner. The bands were competed out by adding **1a** and **2a**, respectively (Figure 5B,F). For analyzing the identity of the bands, the proteins labeled with **P1** or **P2** were coupled with biotin-azide conjugate, enriched by using streptavidin-agarose beads, and analyzed by SDS-PAGE. Silver staining of the enriched proteins also displayed  $\sim 27$  and  $\sim 25$  kDa bands that were competed by **1a** and **2a**, respectively (Figure 5C,G). Western blot analysis of the enriched proteins revealed that the similar  $\sim 27$  and  $\sim 25$  kDa bands were recognized by anti-PGAM1 and anti-GSTP1 antibodies and competed by excess amounts of **1a** and **2a**, respectively (Figure 5D,H). Similar results were obtained when human HeLa and

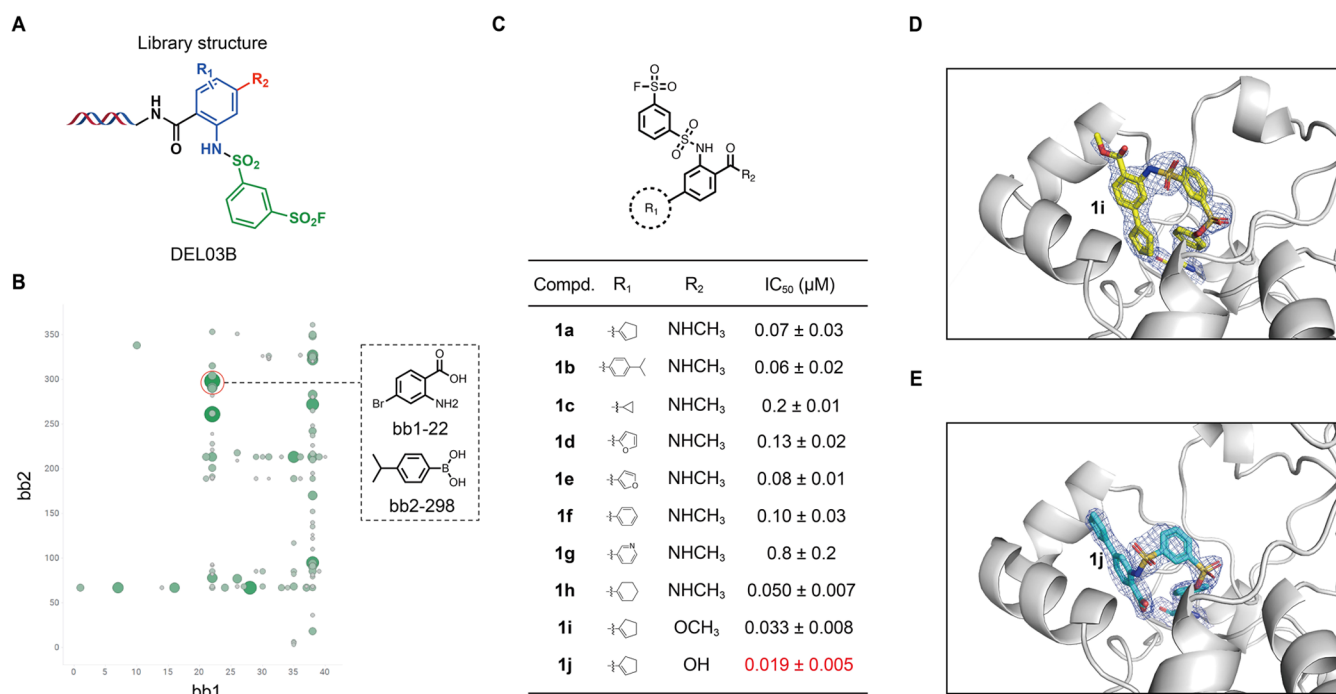


**Figure 6.** Two-cycle focused CoDEL selection against PGAM1. (A) Library structure of a two-cycle focused selection library DEL03B. (B) Selection results are shown as a scatter plot. The resynthesized hit compound is highlighted. (C) SAR study of the off-DNA hit compound from DEL03B. SAR: structure–activity relationship. (D) Crystal structure of **1i** bound to PGAM1 (PDB ID code 7XB9) at a resolution of 1.58 Å. The PGAM1 (gray) is shown as a cartoon, and **1i** (yellow) as sticks. (E) Crystal structure of **1j** bound to PGAM1 (PDB ID code 7XB8) at a resolution of 1.60 Å. The PGAM1 (gray) is shown as a cartoon, and **1j** (blue) as sticks.

HL-60 cell proteomes were used (Figure S13). These results demonstrate the highly selective target engagement of **P1** and **P2** with PGAM1 and GSTP1, respectively.

**Two-Cycle Focused DEL Selection against PGAM1 and Structure–Activity Relationship Study.** Finally, to confirm the stability and repeatability of the SF-based DEL selection, a two-cycle focused library DEL03 was constructed based on cocrystal structure of PGAM1 and **1a** by changing bb1 in cycle 1 to 2-amino-4-halogenated benzoic acid and replacing bb2 with 366 boric acids, primarily with hydrophobic groups, in cycle 2 (Figures 6A and S8). The result of DEL03B selection against PGAM1 stably showed a highly enriched cluster, with cycle 1 being the 2-amino-4-bromobenzoic acid scaffold and cycle 2 being varied phenylboronic acids. We synthesized off-DNA ligand **1b** with the highest fold-enrichment of 29.54 (Figure 6B). The IC<sub>50</sub> value of **1b** was calculated to be 60 nM, which was similar to that of **1a** (Figure 6C). Collectively, these results demonstrate that our library selection is highly reproducible.

The limitation of the encoded compounds imposed by the fixed DNA-conjugated amide groups also encouraged us to adopt a traditional medicinal chemistry approach for derivatizing **1a**. Initially, the cyclopentene group of **1a** was substituted with rings of varying sizes, encompassing both saturated and unsaturated structures. Overall, the resulting analogues exhibited comparable activity to that of **1a**. However, noteworthy improvements in activity were observed upon replacement of the formamide group with a methyl ester (**1i**) or a carboxy group (**1j**), leading to IC<sub>50</sub> values of 33 and 19 nM, respectively (Figure 6C). The cocrystal structure of PGAM1 with **1i** displayed an electrostatic interaction between the methyl ester group and Arg 116 (Figures 6D and S14A). Interestingly, substitution of the formamide group with a

carboxyl group led to a complete alteration in the binding conformation of **1j**. The altered binding mode of **1j** can be attributed to the insertion of the phenyl-cyclopentene scaffold of **1j** into the hydrophobic pocket surrounding Phe 22, Leu 95, and Val 112, along with a robust hydrogen-bonding interaction between the carboxyl group and Arg 90 (Figures 6E and S14B–D).

## CONCLUSIONS

In this study, we developed a screening platform for tyrosine-targeting covalent ligands by integrating SF-based DEL enrichment with activity-based proteome profiling as a guide. Through analyzing the reactivity of sulfonyl fluoride electrophiles in proteomes, we identified the appropriate targets for sulfonyl-fluoride DEL selection. Recently, covalent DEL emerged as a robust covalent ligand discovery technology by incorporation of an electrophile warhead into DNA-encoded compounds. However, the random selection of proteins for irreversible screening might lead to low efficiency and diversity. Proteome profiling-guided covalent DEL selection is expected to accelerate the covalent ligand discovery for proteins with reactive ligandable hotspots.

Our approach provided an efficient method to develop covalent ligands against the proteins with limited information about ligandable hotspots as long as they were labeled by SF probes. We noted that only a covalent probe MJE3 carrying an epoxide group was reported to react with the Lys 100 of PGAM1.<sup>37</sup> GS-ESF, a derivative of GSH terminated with a sulfonyl fluoride group, covalently bound to the Tyr 108 of GSTP1.<sup>38</sup> Another reported inhibitor carrying a cyclopropenone group covalently reacts with Cys 47 of GSTP1.<sup>39</sup> In addition, covalent inhibitors developed for DPP3 have not been reported yet because the development of DPP3 inhibitors

itself is still unsatisfying due to the big substrate binding pocket.<sup>40,41</sup> Based on the current study of the above three proteins, developing covalent ligands with a new mode of action through traditional strategy remains challenging. However, with SF-based DEL selection, we quickly identified the covalent ligands reacting with tyrosine residues that have not been selectively targeted before. It implied that more covalent ligands, which could not be easily achieved by other methods, might be discovered for all of the other SF probe-labeled proteins.

Another advantage of our strategy is the reasonable selectivity of the developed covalent ligands. This is due to the application of sulfonyl fluoride warhead, which reacts with tyrosine in a click-like manner, typically activated through chemically induced proximity effect driven by ligand binding. A variety of ligands with SuFEx warheads were reported to target different residues by rational design, illustrating the incredible diversity of SuFEx chemistry.<sup>42</sup> For DEL construction and screening, the reactivity and stability of the SuFEx electrophiles are key considerations. The aryl-sulfonyl fluorides were chosen to be the warheads of covalent DELs due to their moderate reactivity between alkyl-sulfonyl fluorides and the sulfonimido-fluorides.<sup>43</sup> During the covalent DEL construction, the stability of electrophiles under DNA-compatible reaction conditions in aqueous media was critical, which led the aryl-SFs to be more suitable than alkyl-SFs. Furthermore, compounds incorporating the aryl-SF group confer stronger additional affinity beyond the noncovalent interactions involved in ligand binding than the sulfonimido-fluoride group, which might lead to higher screening efficiency and hit rates. Although the highly reactive SF warheads were proven to be a liability for drug development, the effects of electronic and steric factors on hit compounds can be regulated to generate an optimal balance between reactivity and stability for subsequent optimization.

Although this method led to the discovery of tyrosine-targeted covalent ligands against multiple proteins, it should be further extended and developed. For example, there are additional visible bands, as labeled by P1 and P2 in cell lysates. This is probably due to the limited core scaffolds and chemical spaces in our DEL, which may limit the selectivity of hit compounds. Novel DNA-compatible chemistry and a variety of scaffolds are necessary to develop for further CoDEL screening. One flaw in our method is that a protein should not be subjected to SF-based CoDEL screening if it was not labeled by the SF probes. To strengthen the rationale, we attempted enolase 1, which was not labeled by SF probes, and were unable to acquire hit compounds. It suggested that certain proteins might be excluded from the encoded chemical libraries with a single electrophilic warhead. To solve this problem, more electrophiles should be applied to covalent DEL to extend the diversity and application of DELs. Expansion of our approach to other amino acids with alternative warheads should afford additional opportunities for covalent ligand development in future drug discovery.

## ■ ASSOCIATED CONTENT

### SI Supporting Information

The Supporting Information is available free of charge at <https://pubs.acs.org/doi/10.1021/jacs.3c08852>.

Materials and general methods; SF-based probes labeling experiments; preparation of the DNA-encoded chemical

libraries; chemical synthesis and characterization; target validation of SF-based ligands from DEL selection; and unprocessed gels or blots for figures (Figures S1–S15) (Tables S1 and S2) (PDF)

## ■ AUTHOR INFORMATION

### Corresponding Authors

**Minjia Tan** – State Key Laboratory of Drug Research, Shanghai Institute of Materia Medica, Chinese Academy of Sciences, Shanghai 201203, China; Zhongshan Institute for Drug Discovery, Shanghai Institute of Materia Medica, Chinese Academy of Sciences, Zhongshan, Guangdong 528400, China; [orcid.org/0000-0002-6784-9653](https://orcid.org/0000-0002-6784-9653); Email: [mjtan@simmm.ac.cn](mailto:mjtan@simmm.ac.cn)

**Xiaojie Lu** – State Key Laboratory of Drug Research, Shanghai Institute of Materia Medica, Chinese Academy of Sciences, Shanghai 201203, China; University of Chinese Academy of Sciences, Beijing 100049, China; [orcid.org/0000-0002-3600-288X](https://orcid.org/0000-0002-3600-288X); Email: [xjlu@simmm.ac.cn](mailto:xjlu@simmm.ac.cn)

**Lu Zhou** – School of Pharmacy, Fudan University, Shanghai 201203, China; [orcid.org/0000-0002-6807-2647](https://orcid.org/0000-0002-6807-2647); Email: [zhoulu@fudan.edu.cn](mailto:zhoulu@fudan.edu.cn)

### Authors

**Lulu Jiang** – School of Pharmacy, Fudan University, Shanghai 201203, China

**Sixiu Liu** – State Key Laboratory of Drug Research, Shanghai Institute of Materia Medica, Chinese Academy of Sciences, Shanghai 201203, China; University of Chinese Academy of Sciences, Beijing 100049, China

**Xinglong Jia** – School of Pharmacy, Fudan University, Shanghai 201203, China

**Qinting Gong** – School of Pharmacy, Fudan University, Shanghai 201203, China

**Xin Wen** – State Key Laboratory of Drug Research, Shanghai Institute of Materia Medica, Chinese Academy of Sciences, Shanghai 201203, China; University of Chinese Academy of Sciences, Beijing 100049, China

**Weiwei Lu** – State Key Laboratory of Drug Research, Shanghai Institute of Materia Medica, Chinese Academy of Sciences, Shanghai 201203, China

**Jintong Yang** – School of Pharmacy, Fudan University, Shanghai 201203, China

**Xinyuan Wu** – State Key Laboratory of Drug Research, Shanghai Institute of Materia Medica, Chinese Academy of Sciences, Shanghai 201203, China; University of Chinese Academy of Sciences, Beijing 100049, China

**Xuan Wang** – State Key Laboratory of Drug Research, Shanghai Institute of Materia Medica, Chinese Academy of Sciences, Shanghai 201203, China; [orcid.org/0000-0003-4986-0231](https://orcid.org/0000-0003-4986-0231)

**Yanrui Suo** – State Key Laboratory of Drug Research, Shanghai Institute of Materia Medica, Chinese Academy of Sciences, Shanghai 201203, China; University of Chinese Academy of Sciences, Beijing 100049, China

**Yilin Li** – National Facility for Protein Science in Shanghai, Shanghai Advanced Research Institute, Chinese Academy of Science, Shanghai 201210, China

**Motonari Uesugi** – School of Pharmacy, Fudan University, Shanghai 201203, China; Institute for Chemical Research and Institute for Integrated Cell-Material Sciences (WPI-iCeMS), Kyoto University, Uji, Kyoto 611-0011, Japan; [orcid.org/0000-0002-8515-445X](https://orcid.org/0000-0002-8515-445X)

Zhi-bei Qu – School of Pharmacy, Fudan University, Shanghai 201203, China; [orcid.org/0000-0003-1517-0822](https://orcid.org/0000-0003-1517-0822)

Complete contact information is available at: <https://pubs.acs.org/10.1021/jacs.3c08852>

### Author Contributions

<sup>○</sup>L.J., S.L., and X.J. contributed equally. L.Z., X.L., and M.T. contributed to the central experimental idea. L.J., S.L., X.J., Q.G., X.W., W.L., J.Y., X.W., X.W., Y.S., and Y.L. designed and performed the experiments. L.J. wrote the original draft. L.Z., X.L., M.T., M.U., and Z.Q. supervised the project, revised the manuscript, and commented on it.

### Notes

The authors declare no competing financial interest.

<sup>▽</sup>Lead Contact.

## ACKNOWLEDGMENTS

The authors thank the staff at beamline BL17U, BL18U1, and BL19U1 at the Shanghai Synchrotron Radiation Facility (SSRF) for supporting with data collection. The protein mass analysis is supported by the National Center for Protein Science Shanghai. Work in L.Z.'s laboratory is supported by the National Natural Science Foundation of China (no. 22077019) and Shanghai Municipal Committee of Science and Technology (nos. 21TQ016 and 21XD1420600). Work in X.L.'s laboratory is supported by National Natural Science Foundation of China (nos. 91953203 and 92253305). Work in M.T.'s laboratory is supported by National Natural Science Foundation of China (nos. 22225702 and 92153302) and Shanghai Municipal Committee of Science and Technology (no. 22XD1420900). This work was partially supported and inspired by the International Collaborative Research Program of Institute for Chemical Research, Kyoto University (grant no. 2022-94), Kyoto University On-Site Lab (Fudan-Kyoto Shanghai Lab), and the international and interdisciplinary environments of JSPS CORE-to-CORE Program 'Asian Chemical Biology Initiative'.

## REFERENCES

- (1) Zhang, T.; Hatcher, J. M.; Teng, M.; Gray, N. S.; Kostic, M. Recent Advances in Selective and Irreversible Covalent Ligand Development and Validation. *Cell Chem. Biol.* **2019**, *26* (11), 1486–1500.
- (2) Boike, L.; Henning, N. J.; Nomura, D. K. Advances in covalent drug discovery. *Nat. Rev. Drug Discovery* **2022**, *21* (12), 881–898.
- (3) Soria, J. C.; Felip, E.; Cobo, M.; Lu, S.; Syrigos, K.; Lee, K. H.; Goker, E.; Georgoulas, V.; Li, W.; Isla, D.; Guclu, S. Z.; Morabito, A.; Min, Y. J.; Ardizzoni, A.; Gadgeel, S. M.; Wang, B.; Chand, V. K.; Goss, G. D.; Investigators, L. U.-L. Afatinib versus erlotinib as second-line treatment of patients with advanced squamous cell carcinoma of the lung (LUX-Lung 8): an open-label randomised controlled phase 3 trial. *Lancet Oncol.* **2015**, *16* (8), 897–907.
- (4) Byrd, J. C.; Furman, R. R.; Coutre, S. E.; Flinn, I. W.; Burger, J. A.; Blum, K. A.; Grant, B.; Sharman, J. P.; Coleman, M.; Wierda, W. G.; Jones, J. A.; Zhao, W.; Heerema, N. A.; Johnson, A. J.; Sukbuntherng, J.; Chang, B. Y.; Clow, F.; Hedrick, E.; Buggy, J. J.; James, D. F.; O'Brien, S. Targeting BTK with ibrutinib in relapsed chronic lymphocytic leukemia. *N Engl J. Med.* **2013**, *369* (1), 32–42.
- (5) Wang, M. L.; Rule, S.; Martin, P.; Goy, A.; Auer, R.; Kahl, B. S.; Jurczak, W.; Advani, R. H.; Romaguera, J. E.; Williams, M. E.; Barrientos, J. C.; Chmielowska, E.; Radford, J.; Stilgenbauer, S.; Dreyling, M.; Jdrzejczak, W. W.; Johnson, P.; Spurgeon, S. E.; Li, L.; Zhang, L.; Newberry, K.; Ou, Z.; Cheng, N.; Fang, B.; McCreivy, J.; Clow, F.; Buggy, J. J.; Chang, B. Y.; Beaupre, D. M.; Kunkel, L. A.; Blum, K. A. Targeting BTK with ibrutinib in relapsed or refractory mantle-cell lymphoma. *N Engl J. Med.* **2013**, *369* (6), 507–516.
- (6) Huang, L.; Guo, Z.; Wang, F.; Fu, L. KRAS mutation: from undruggable to druggable in cancer. *Signal Transduction Targeted Ther.* **2021**, *6* (1), 386.
- (7) Moore, A. R.; Rosenberg, S. C.; McCormick, F.; Malek, S. RAS-targeted therapies: is the undruggable drugged? *Nat. Rev. Drug Discovery* **2020**, *19* (8), 533–552.
- (8) Lu, W.; Kostic, M.; Zhang, T.; Che, J.; Patricelli, M. P.; Jones, L. H.; Chouchani, E. T.; Gray, N. S. Fragment-based covalent ligand discovery. *RSC Chem. Biol.* **2021**, *2* (2), 354–367.
- (9) Lagoutte, R.; Patouret, R.; Winssinger, N. Covalent inhibitors: an opportunity for rational target selectivity. *Curr. Opin. Chem. Biol.* **2017**, *39*, 54–63.
- (10) Lonsdale, R.; Ward, R. A. Structure-based design of targeted covalent inhibitors. *Chem. Soc. Rev.* **2018**, *47* (11), 3816–3830.
- (11) Metcalf, B.; Chuang, C.; Dufu, K.; Patel, M. P.; Silva-Garcia, A.; Johnson, C.; Lu, Q.; Partridge, J. R.; Patskovska, L.; Patskovsky, Y.; Almo, S. C.; Jacobson, M. P.; Hua, L.; Xu, Q.; Gwaltney, S. L., 2nd; Yee, C.; Harris, J.; Morgan, B. P.; James, J.; Xu, D.; Hutchaleelaha, A.; Paulvannan, K.; Oksenberg, D.; Li, Z. Discovery of GBT440, an Orally Bioavailable R-State Stabilizer of Sick Cell Hemoglobin. *ACS Med. Chem. Lett.* **2017**, *8* (3), 321–326.
- (12) Arasappan, A.; Bennett, F.; Bogen, S. L.; Venkatraman, S.; Blackman, M.; Chen, K. X.; Hendrata, S.; Huang, Y.; Huelgas, R. M.; Nair, L.; Padilla, A. I.; Pan, W.; Pike, R.; Pinto, P.; Ruan, S.; Sannigrahi, M.; Velazquez, F.; Vibulbhan, B.; Wu, W.; Yang, W.; Saksena, A. K.; Girijavallabhan, V.; Shih, N. Y.; Kong, J.; Meng, T.; Jin, Y.; Wong, J.; McNamara, P.; Prongay, A.; Madison, V.; Piwinski, J. J.; Cheng, K. C.; Morrison, R.; Malcolm, B.; Tong, X.; Ralston, R.; Njoroge, F. G. Discovery of Narlaprevir (SCH 900518): A Potent, Second Generation HCV NS3 Serine Protease Inhibitor. *ACS Med. Chem. Lett.* **2010**, *1* (2), 64–69.
- (13) Curran, M. P.; McKeage, K. Bortezomib: a review of its use in patients with multiple myeloma. *Drugs* **2009**, *69* (7), 859–888.
- (14) Huang, Y.; Li, Y.; Li, X. Strategies for developing DNA-encoded libraries beyond binding assays. *Nat. Chem.* **2022**, *14* (2), 129–140.
- (15) Neri, D.; Lerner, R. A. DNA-Encoded Chemical Libraries: A Selection System Based on Endowing Organic Compounds with Amplifiable Information. *Annu. Rev. Biochem.* **2018**, *87*, 479–502.
- (16) Lerner, R. A.; Brenner, S. DNA-Encoded Compound Libraries as Open Source: A Powerful Pathway to New Drugs. *Angew. Chem., Int. Ed.* **2017**, *56* (5), 1164–1165.
- (17) Brenner, S.; Lerner, R. A. Encoded combinatorial chemistry. *Proc. Natl. Acad. Sci. U.S.A.* **1992**, *89* (12), 5381–5383.
- (18) Debaene, F.; Mejias, L.; Harris, J. L.; Winssinger, N. Synthesis of a PNA-encoded cysteine protease inhibitor library. *Tetrahedron* **2004**, *60* (39), 8677–8690.
- (19) Urbina, H. D.; Debaene, F.; Jost, B.; Bole-Feysot, C.; Mason, D. E.; Kuzmic, P.; Harris, J. L.; Winssinger, N. Self-assembled small-molecule microarrays for protease screening and profiling. *Chem-biochem* **2006**, *7* (11), 1790–1797.
- (20) Debaene, F.; Da Silva, J. A.; Pianowski, Z.; Duran, F. J.; Winssinger, N. Expanding the scope of PNA-encoded libraries: divergent synthesis of libraries targeting cysteine, serine and metalloproteases as well as tyrosine phosphatases. *Tetrahedron* **2007**, *63* (28), 6577–6586.
- (21) Zambaldo, C.; Daguier, J. P.; Saabach, J.; Barluenga, S.; Winssinger, N. Screening for covalent inhibitors using DNA-display of small molecule libraries functionalized with cysteine reactive moieties. *MedChemComm* **2016**, *7* (7), 1340–1351.
- (22) Daguier, J. P.; Zambaldo, C.; Abegg, D.; Barluenga, S.; Tallant, C.; Muller, S.; Adibekian, A.; Winssinger, N. Identification of Covalent Bromodomain Binders through DNA Display of Small Molecules. *Angew. Chem., Int. Ed.* **2015**, *54* (20), 6057–6061.
- (23) Guilinger, J. P.; Archana, A.; Augustin, M.; Bergmann, A.; Centrella, P. A.; Clark, M. A.; Cuozzo, J. W.; Dather, M.; Guie, M. A.; Habeshian, S.; Kiefersauer, R.; Krapp, S.; Lammens, A.; Lercher, L.;

- Liu, J.; Liu, Y.; Maskos, K.; Mrosek, M.; Pflugler, K.; Siegert, M.; Thomson, H. A.; Tian, X.; Zhang, Y.; Konz Makino, D. L.; Keefe, A. D. Novel irreversible covalent BTK inhibitors discovered using DNA-encoded chemistry. *Bioorg. Med. Chem.* **2021**, *42*, No. 116223.
- (24) Li, L.; Su, M.; Lu, W.; Song, H.; Liu, J.; Wen, X.; Suo, Y.; Qi, J.; Luo, X.; Zhou, Y. B.; Liao, X. H.; Li, J.; Lu, X. Triazine-Based Covalent DNA-Encoded Libraries for Discovery of Covalent Inhibitors of Target Proteins. *ACS Med. Chem. Lett.* **2022**, *13* (10), 1574–1581.
- (25) Zimmermann, G.; Rieder, U.; Bajic, D.; Vanetti, S.; Chaikuad, A.; Knapp, S.; Scheuermann, J.; Mattarella, M.; Neri, D. A Specific and Covalent JNK-1 Ligand Selected from an Encoded Self-Assembling Chemical Library. *Chem. – Eur. J.* **2017**, *23* (34), 8152–8155.
- (26) Ge, R.; Shen, Z.; Yin, J.; Chen, W.; Zhang, Q.; An, Y.; Tang, D.; Satz, A. L.; Su, W.; Kuai, L. Discovery of SARS-CoV-2 main protease covalent inhibitors from a DNA-encoded library selection. *SLAS Discovery* **2022**, *27* (2), 79–85.
- (27) Fadeyi, O. O.; Hoth, L. R.; Choi, C.; Feng, X.; Gopalsamy, A.; Hett, E. C.; Kyne, R. E., Jr.; Robinson, R. P.; Jones, L. H. Covalent Enzyme Inhibition through Fluorosulfate Modification of a Non-catalytic Serine Residue. *ACS Chem. Biol.* **2017**, *12* (8), 2015–2020.
- (28) Li, S. H.; Cohen-Karni, D.; Beringer, L. T.; Wu, C. G.; Kallick, E.; Edington, H.; Passineau, M. J.; Averick, S. Direct introduction of R-SO<sub>2</sub>F moieties into proteins and protein-polymer conjugation using SuFEx chemistry. *Polymer* **2016**, *99*, 7–12.
- (29) Hett, E. C.; Xu, H.; Geoghegan, K. F.; Gopalsamy, A.; Kyne, R. E., Jr.; Menard, C. A.; Narayanan, A.; Parikh, M. D.; Liu, S.; Roberts, L.; Robinson, R. P.; Tones, M. A.; Jones, L. H. Rational targeting of active-site tyrosine residues using sulfonyl fluoride probes. *ACS Chem. Biol.* **2015**, *10* (4), 1094–1098.
- (30) Zheng, Q.; Woehl, J. L.; Kitamura, S.; Santos-Martins, D.; Smedley, C. J.; Li, G.; Forli, S.; Moses, J. E.; Wolan, D. W.; Sharpless, K. B. SuFEx-enabled, agnostic discovery of covalent inhibitors of human neutrophil elastase. *Proc. Natl. Acad. Sci. U.S.A.* **2019**, *116* (38), 18808–18814.
- (31) Dong, J.; Krasnova, L.; Finn, M. G.; Sharpless, K. B. Sulfur(VI) fluoride exchange (SuFEx): another good reaction for click chemistry. *Angew. Chem., Int. Ed.* **2014**, *53* (36), 9430–9448.
- (32) Yan, T.; Desai, H. S.; Boatner, L. M.; Yen, S. L.; Cao, J.; Palafox, M. F.; Jami-Alahmadi, Y.; Backus, K. M. SP3-FAIMS Chemoproteomics for High-Coverage Profiling of the Human Cysteineome\*. *Chembiochem* **2021**, *22* (10), 1841–1851.
- (33) Hahm, H. S.; Toroitich, E. K.; Borne, A. L.; Brulet, J. W.; Libby, A. H.; Yuan, K.; Ware, T. B.; McCloud, R. L.; Ciancone, A. M.; Hsu, K. L. Global targeting of functional tyrosines using sulfur-triazole exchange chemistry. *Nat. Chem. Biol.* **2020**, *16* (2), 150–159.
- (34) Cravatt, B. F.; Wright, A. T.; Kozarich, J. W. Activity-based protein profiling: from enzyme chemistry to proteomic chemistry. *Annu. Rev. Biochem.* **2008**, *77*, 383–414.
- (35) Backus, K. M.; Correia, B. E.; Lum, K. M.; Forli, S.; Horning, B. D.; Gonzalez-Paez, G. E.; Chatterjee, S.; Lanning, B. R.; Teijaro, J. R.; Olson, A. J.; Wolan, D. W.; Cravatt, B. F. Proteome-wide covalent ligand discovery in native biological systems. *Nature* **2016**, *534* (7608), 570–574.
- (36) Wishart, D. S.; Feunang, Y. D.; Guo, A. C.; Lo, E. J.; Marcu, A.; Grant, J. R.; Sajed, T.; Johnson, D.; Li, C.; Sayeeda, Z.; Assempour, N.; Iynkkaran, I.; Liu, Y.; Maciejewski, A.; Gale, N.; Wilson, A.; Chin, L.; Cummings, R.; Le, D.; Pon, A.; Knox, C.; Wilson, M. DrugBank 5.0: a major update to the DrugBank database for 2018. *Nucleic Acids Res.* **2018**, *46* (D1), D1074–D1082.
- (37) Evans, M. J.; Morris, G. M.; Wu, J.; Olson, A. J.; Sorensen, E. J.; Cravatt, B. F. Mechanistic and structural requirements for active site labeling of phosphoglycerate mutase by spiroepoxides. *Mol. Biosyst.* **2007**, *3* (7), 495–506.
- (38) Shishido, Y.; Tomoike, F.; Kimura, Y.; Kuwata, K.; Yano, T.; Fukui, K.; Fujikawa, H.; Sekido, Y.; Murakami-Tonami, Y.; Kameda, T.; Shuto, S.; Abe, H. A covalent G-site inhibitor for glutathione S-transferase Pi (GSTP(1–1)). *Chem. Commun.* **2017**, *53* (81), 11138–11141.
- (39) Fan, Y.; Si, H.; Zhang, Z.; Zhong, L.; Sun, H.; Zhu, C.; Yin, Z.; Li, H.; Tang, G.; Yao, S. Q.; Sun, P.; Zhang, Z. M.; Ding, K.; Li, Z. Novel Electrophilic Warhead Targeting a Triple-Negative Breast Cancer Driver in Live Cells Revealed by “Inverse Drug Discovery”. *J. Med. Chem.* **2021**, *64* (21), 15582–15592.
- (40) Bezerra, G. A.; Dobrovetsky, E.; Viertlmayr, R.; Dong, A.; Binter, A.; Abramic, M.; Macheroux, P.; Dhe-Paganon, S.; Gruber, K. Entropy-driven binding of opioid peptides induces a large domain motion in human dipeptidyl peptidase III. *Proc. Natl. Acad. Sci. U.S.A.* **2012**, *109* (17), 6525–6530.
- (41) Kumar, P.; Reithofer, V.; Reisinger, M.; Wallner, S.; Pavkov-Keller, T.; Macheroux, P.; Gruber, K. Substrate complexes of human dipeptidyl peptidase III reveal the mechanism of enzyme inhibition. *Sci. Rep* **2016**, *6*, No. 23787.
- (42) Huang, H.; Jones, L. H. Covalent drug discovery using sulfur(VI) fluoride exchange warheads. *Expert Opin. Drug Discovery* **2023**, *18* (7), 725–735.
- (43) Mukherjee, H.; Debreczeni, J.; Breed, J.; Tentarelli, S.; Aquila, B.; Dowling, J. E.; Whitty, A.; Grimster, N. P. A study of the reactivity of S(VI)-F containing warheads with nucleophilic amino-acid side chains under physiological conditions. *Org. Biomol. Chem.* **2017**, *15* (45), 9685–9695.